Landslides
DOI 10.1007/s10346-016-0705-7
Received: 18 December 2015
Accepted: 17 March 2016

Edouard Palis · Thomas Lebourg · Emmanuel Tric · Jean-Philippe Malet · Maurin Vidal

Long-term monitoring of a large deep-seated landslide (La Clapiere, South-East French Alps): initial study

Abstract The large-scale deformation of high mountain slopes finds its origin in many phenomena (inherent parameters, external stresses) with very different time constants (instantaneous to geological scale). Gravitational effect, tectonic forces and water infiltration are generally the principal causes of slope instability. However, it can be very difficult to distinguish which cause is dominant and which are their respective effects. To gain a better understanding of the complex processes taking place during the evolution of an unstable slope and separate the causes responsible of the landslide dynamic, an observational study based on geodetic, meteorological, seismological and electrical data has been performed on the La Clapière rockslide (Southern French Alps). This deep-seated landslide (DSL) is known for many years as one of the largest and fastest rock slide in Europe (60 million m^3 of highly weathered metamorphic material, moving at 1 to 3 m $year^{-1}$). The set-up of the "Observatoire Multidisciplinaire des Instabilités de Versants" (OMIV, http://omiv.osug.fr) in 2011 has allowed the production and availability of an important and original data set over several years of accurate monitoring. Thus, for the first time, the long-term study of geodetic data permitted us to highlight acceleration phases in the general movement of the landslide that affect its dynamic. These modifications are associated with variations of the velocity by a factor 3 to 6. The characterization of the origin of these variations was possible due to the comparison with meteorological, electrical and seismological data. Based on these various signals, we were able to establish correlations and contributions of meteorological water infiltration in the dynamic evolution of the La Clapière slope. We determine several response times to the meteorological stress for seismic endogenous events (mainly rockfalls), the resistivity of the ground (quasi-instantaneous) and the kinematics of the slope (from 2 weeks to 2.5 months). Moreover, our results strongly suggest the existence of rainfall threshold of 3.5 ± 1 mm day^{-1} from which the number of seismic endogenous events is highly increased.

Keywords La Clapière · Landslide monitoring · Multi-parameter analysis · Electrical resistivity tomography

Introduction

The landslide process is the main shallow consequence of mountain slope erosion, result of tectonic heritage and climatic history. Understanding landslide processes and their precursor parameters is a real challenge for scientists and for society. Many factors and a long history influence the evolution of a slope deformation. For many years, scientists have tried to study and understand the features of landslides, as well as the causes of their triggering and evolution.

Many authors have tried to characterize the geology and the geometry of several landslides using different methods (Varnes 1978; Jongmans and Garambois 2007; Korup et al. 2010; Jaboyedoff et al. 2012; Schlögel et al. 2015a), their kinematics (Delacourt et al. 2007; Korup et al. 2007), as well as their triggering factors (Crosta 1998; Keefer 2002). Multi-year, multi-parameter monitoring is a promising approach, which has recently been applied in several studies (Macfarlane 2009; Helmstetter and Garambois 2010; Mainsant et al. 2012; Crosta et al. 2014; Prokešová et al. 2014).

Partly due to a significant glacial history, the very fractured and weathered northern part of the Tinée Valley, in the western part of the Mercantour-Argentera massif in the French Alps, is very susceptible to landslides. Previous studies have revealed the existence of major deep-seated deformation affecting tens of kilometres along the north bank of the valley (Jomard 2006; El Bedoui et al. 2009, 2011; Jomard et al. 2013). The La Clapière landslide, considered to be one of the most active deep-seated landslides (DSLs) in Europe, is a shallow response to this deep-seated gravitational slope deformation (DSGSD). Situated downstream of the Saint-Etienne-de-Tinée village, the landslide represents an important risk and therefore a high-priority scientific challenge.

The objective of this work is to analyse multi-parameter observational data of La Clapière landslide, an important rockslide monitored from the 1980s. For the first time, more than 4 years of accurate daily data are compiled to characterize short-term features.

This well-known rockslide, based on Varnes 1978's classification system, has been the subject of numerous studies (Bogdanoff 1980; Julian and Anthony 1996; Musumeci et al. 2003; Bois et al. 2008; Guglielmi and Cappa 2010; El Bedoui et al. 2011; Jomard et al. 2013; Bois et al. 2014). Authors have discussed the past and active tectonic dynamics of the area (Bogdanoff 1980; Gunzburger and Laumonier 2002; Musumeci et al. 2003), as well as the erosive effects of climate on the valley (Julian and Anthony 1996). Some works chronologically constraining the evolution of the slope have also been performed (Corsini et al. 2004; Bigot-Cormier et al. 2005; El Bedoui et al. 2009, 2011). Finally, thanks to long-term surveys and monitoring data that we are now able to produce, models of deformation have been produced (Cappa et al. 2004; Bois et al. 2008; Tric et al. 2010; El Bedoui et al. 2011). However, none of these studies have integrated the monitoring of several forcing and measurable parameters over an accurate period of time.

To understand the behaviour of this DSL, scientists (CNRS-INSU, CETE Meditéranée, OMIV) installed progressively a dense instrumentation with several permanent stations measuring the weather conditions at different locations, the displacement of geodetic points (global positioning system (GPS) and targets), the electrical resistivity of the ground at the foot of the slope (electrical resistivity tomography (ERT)), the chemistry of two springs within the landslide and the slide quakes identified by seismological sensors.

In this work, we aim to present the time series of the data set from OMIV Observatory, as a result of numerous years of accurate monitoring, and to propose an explanation of the time delay between the different measured parameters. For the first time, we use jointly these observations (displacement, meteorology,

Published online: 12 April 2016

endogenous seismological events and electrical resistivity tomography) to characterize the dynamic nature of the unstable slope of La Clapière.

General settings of the study area

The unstable slope La Clapière (approximately 60 million m^3 of material moving over more than 80 ha), constituted of highly fractured material, is located in the north-western part of the Mercantour-Argentera crystalline massif, in the French Southern Alps, on the left bank of the Tinée River. Oriented north-west–south-east, the area is delimited by the Tenibres River (NW) and the Rabuons River (SE) (Fig. 1).

This important rockslide is affected by numerous crack faults and inherited reactivated faults. The valley landscape results from both old tectonic stresses (Varisc to Alpine) and Quaternary climatic fluctuations. During the recent period (Pliocene to present), tectonic activity in the area linked to the uplift of the Argentera massif has been noted. As a consequence of south-westward thrusting along the Variscan myolinitic shear zone in the central part of the massif, this tectonic activity affects the morphology of all of the surrounding valleys (Musumeci et al. 2003; Corsini et al. 2004). Denudation speeds from geo-chronological studies have been estimated at 0.25 mm $year^{-1}$ for the period from −8 to −3.5 Ma and approximately 1 mm $year^{-1}$ for the period from −3.5 Ma to the present (Bogdanoff et al. 2000; Bigot-Cormier et al. 2000, 2005, 2006; El Bedoui et al. 2011). Then, the succession of glacial and interglacial periods, and more precisely, the regional Würmian glacier, has highly modified the landscape (Julian 1980). This glacial erosion may have structured the flanks of the valley in its present state (Julian and Anthony 1996).

This particular topographic heritage has led to some major gravitational deformations that are recognizable from specific structures; double crests, counterscarps and scarps (from the top to the bottom of the slope) are evidences of DSGSD that affects tens of kilometres along the Tinée River (Jomard 2006; El Bedoui et al. 2011; Jomard et al. 2013). These major deformations are constrained by two main directions: N 110°–130° (foliations, faults) and N 010°–030° (collision faults during the Alpine phase). Moreover, following El Bedoui et al. (2009, 2011), the study of the cracks and trenches located on the slope has led to the identification of three phases of evolution respectively controlled by tectonic activity, climate and seasonal fluctuations: (i) tectonic opening of trenches over a large scale and long period (4 mm $year^{-1}$ from 10 to 5.6 ky BP); (ii) shearing of trenches over a shorter period, due to climatic variations (13 to 30 mm $year^{-1}$, from 5.6 to 3.6 ky BP) and (iii) rapid (seasonal scale) failure at the foot of the slope with a high displacement rate (>80 mm $year^{-1}$ from 3.5 ky BP to present).

La Clapière landslide, which is part of the Colle Longue DSGSD, also cuts trenches observed within the slope and confirms the existence of a deformation existing before the setting of the destabilization. In fact, these gravitational deformations affect all of the weathered metamorphic material (over more than 100 m deep), of the upper Tinée Valley from the middle of the slope to the crest, while the foot of the slope is affected by active landslides (Jomard 2006; Guglielmi and Cappa 2010; El Bedoui et al. 2011).

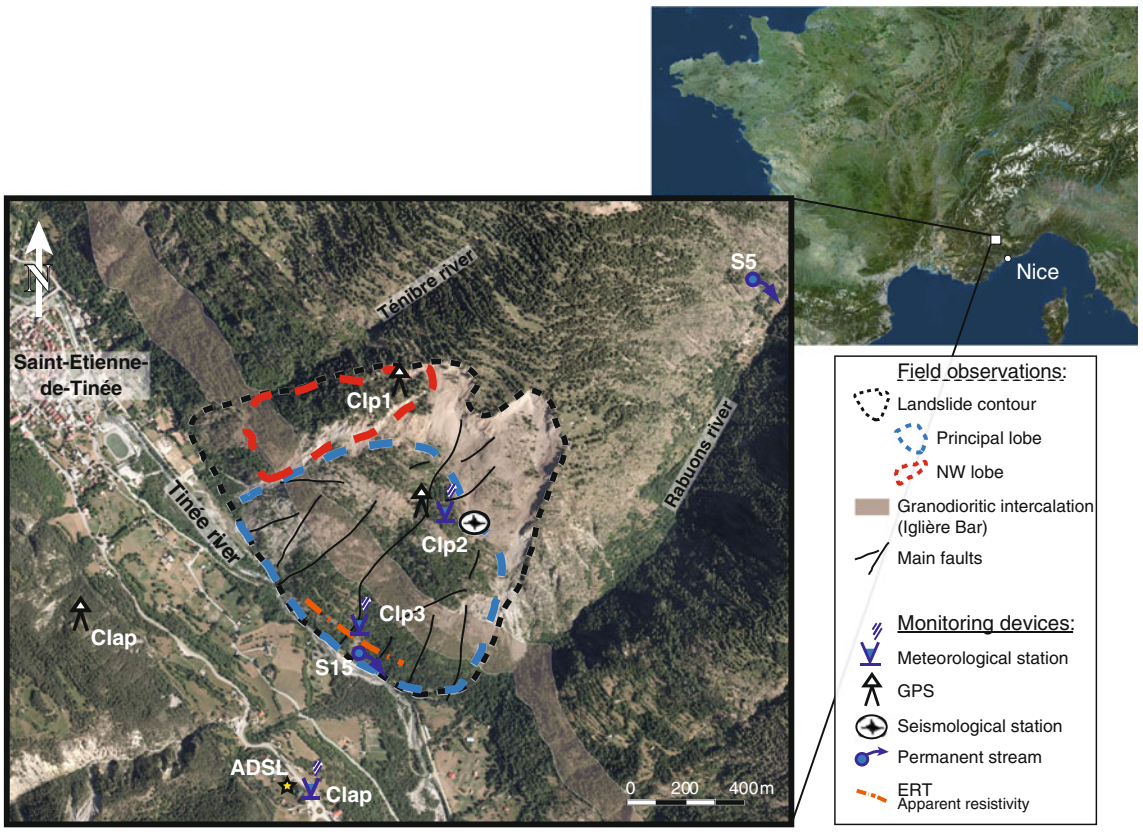

Fig. 1 Location of the study site and the permanent stations installed by the OMIV observatory (station altitudes: CLAP = 1213 m (*star*), CLP2 = 1433 m and CLP3 = 1125 m)

La Clapière DSL, located between 1100 and 1800 m elevation, is constituted of a very weathered Hercynian metamorphic material. Two formations are identified: the Anelle series, consisting of migmatitic gneiss, and the Iglière bar of granodiorite at approximately 250 m from the foot of the slope. The foliation has undergone repeated orogeny and seems to be subhorizontal in this area. Thus, the presence of the Iglière bar provides a resistant support for the slope, whose evolution can allow different behaviours over time.

Thus, the road at the foot of the slope is now entirely covered by landslide's deposits, and the residential areas nearby are strictly forbidden. As a consequence, this landslide had a substantial impact on the village of Saint-Etienne-de-Tinée and hence on the whole Tinée Valley, which is one of the main tributaries of the Var River. These aspects have motivated further studies to investigate the landsliding kinematics by establishing permanent monitoring of benchmarks within the landslide for a period of 33 years (Follacci 1987; Helmstetter et al. 2004; Cappa et al. 2004; Schlögel et al. 2015b). The displacement of these benchmarks has shown important crisis phases from 1982 to the present day (1986–1988, 1997, 2001). The surface motion is now recorded thanks to permanent GPS stations (2013) (Fig. 2).

Regarding these events, numerous authors have contributed to the understanding of the La Clapière landslide by studying the hydrogeology of the slope (Compagnon et al. 1997; Guglielmi et al. 2002; Cappa et al. 2004; Binet et al. 2007) and the geometry of the sliding mass (Jomard et al. 2010; Tric et al. 2010). Finally, works based on electrical resistivity tomography (Lebourg et al. 2005), mechanical behaviour (Lebourg et al. 2011) or optical/radar remote sensing (Casson et al. 2003; Booth et al. 2013; Schlögel et al. 2015b) have addressed the temporal evolution model of the La Clapière DSL.

These major destabilizations must be related to the behaviour of the Iglière bar (Follacci et al. 1993; Guglielmi et al. 2002; Helmstetter et al. 2004). Since then, the slope of La Clapière has been sliding downwards, towards the Tinée River, with active peaks of accelerated movement. Moreover, the very weathered and fractured nature of the substrate implies a major role of meteorological water infiltration (rainfall, snow melt) affecting the equilibrium state of the slope (Fig. 3).

The F2 fault cutting the Iglière bar would be the driving force of these dramatic events. The F1 fault, which acts on the upper part of the landslide, seems to participate to the deceleration of the landslide velocity before converging as listric fault which corresponds to the sliding surface (Follacci et al. 1993; Guglielmi et al. 2002). The fluids coming from rainfalls and/or snow melt infiltrate inside the weathered body and along the main faults and cracks until reaching the S15 permanent stream identified at the landslide foot.

Methods of observation

Multi-parametric approach

By means of the measuring stations we dispose, we are able to observe the unstable slope of La Clapière as a dynamic physical system (Fig. 4). Factors entering the system (inputs), which is characterized by intrinsic variables, and signals coming out of the system can be measured (outputs). Analysing the outputs allows us to gain a better understanding of the way these inputs are integrated into the internal medium (slope system) and thus how they influence the landslide.

Then, measuring and quantifying some of the inputs entering from external environment into the internal medium and identifying some of the resulting output signals can help us to understand the equilibrium state of the open slope system.

OMIV Observatory

In 2007, the French National Institute of Sciences of the Universe (INSU) created the OMIV Observatory (Observatoire Multidisciplinaire des Instabilités de Versant, http://omiv.unice.fr/ ; http://omiv.osug.fr/ ; http://omiv.unistra.fr/) to monitor major

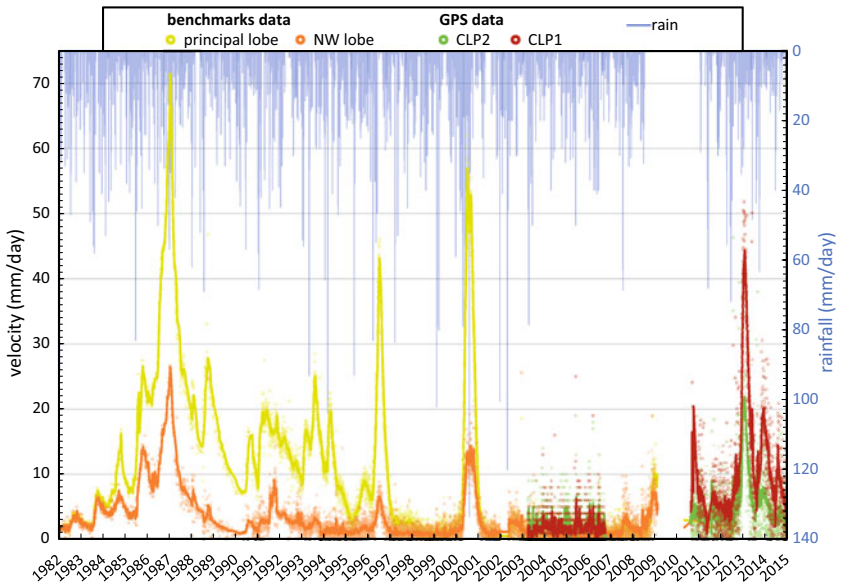

Fig. 2 Evolution of the velocity trends of two parts of the landslide (see Fig. 1 for location) with daily rainfalls recorded at Saint-Etienne-de-Tinée over 33 years (data from *Meteo-France* for the 1967–2008 period and from OMIV from 2010 to 2015). *Lines* show the evolution of average speed. The velocity time series is constructed from previous studies (Follacci 1987; Helmstetter et al. 2004; Schlögel et al. 2015b) for the benchmark data (data from CEREMA); GPS data are detailed in 4.1 section (data from OMIV)

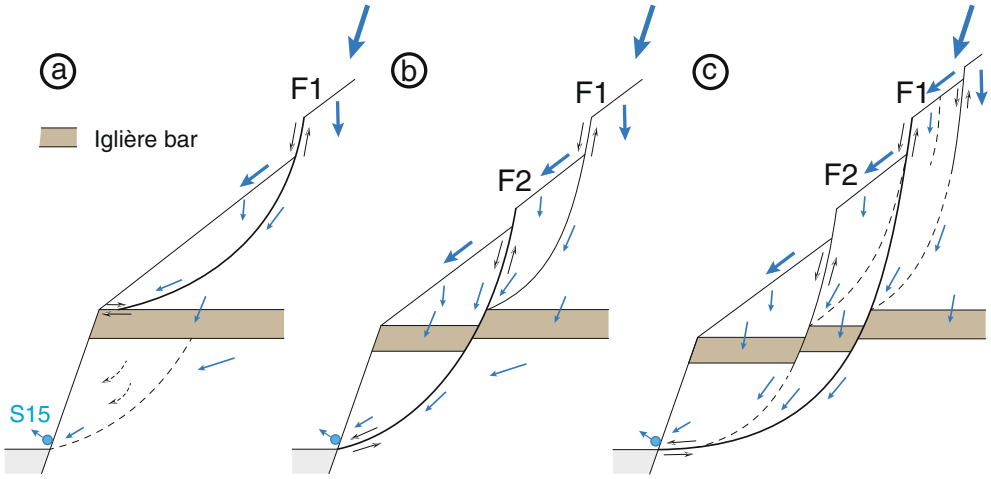

Fig. 3 Schematic failure scenario of the possible process involved in the acceleration crises (adapted from Helmstetter et al. 2004) and the preferential pathways of infiltrated meteorological waters (*blue arrows*). **a** Before event, **b** during the acceleration and **c** after the event

landslides in the French Alps, each of them having a minimum of 10 years of data history. The main objectives of this observatory are to provide specific and accessible data sets that allow us to identify the physical processes that govern slope instability, to model them and to extract the patterns that characterize changes in the landsliding activity. La Clapière, managed by Géoazur, includes four permanent and self-powered stations (Fig. 1):

- On the opposite slope (south bank of the Tinée River):
  - CLAP: GPS (west point), meteorological station, tachometer, internet antenna access (east point)
- Within the landslide body:
  - CLP1 (north-west lobe): GPS
  - CLP2 (principal lobe): GPS, meteorological station, seismological network
  - CLP3 (foot): meteorological station, ERT line

Sampling and physicochemical measurements of permanent streams at the foot of the slope (S15) and upstream of the Rabuons tributary (S5) are also provided (Fig. 1). However, because of the active aspect of the landslide and the very weathered lithology of the deeper layers, no borehole or seismic refraction systems can be installed.

Geodetic equipment

Since 2003, the landslide has been equipped with three permanent GPS stations: two within the landslide body and one on the opposite slope, on the southern bank of the Tinée Valley, which is assumed to be stable (Fig. 1).

GPS data are acquired daily at acquisition rates of 30 and 1 s, and the observations are produced and transmitted by a wireless access point within 1 day. This allows the visualization of the relative displacement with 1-mm precision in near real time.

The OMIV GPS observations are processed using a precise point positioning (PPP) approach which consists in calculating the positions for a single GPS receiver in a dynamic and global reference spatial framework. PPP combines precise clocks and orbits calculated from a global network to calculate a precise position with a single receiver which can be double or single frequency. It differs from classical dual difference (DD) positioning methods which differentiate errors using one or more reference stations with known positions. At La Clapière, the GNSS receivers are CLAP, CLP1 and CLP2 (Fig. 1). After conversion of the raw observations in the standard RINEX observation file formats (e.g. 24 h/30 s), a precise position in ITRF 2008

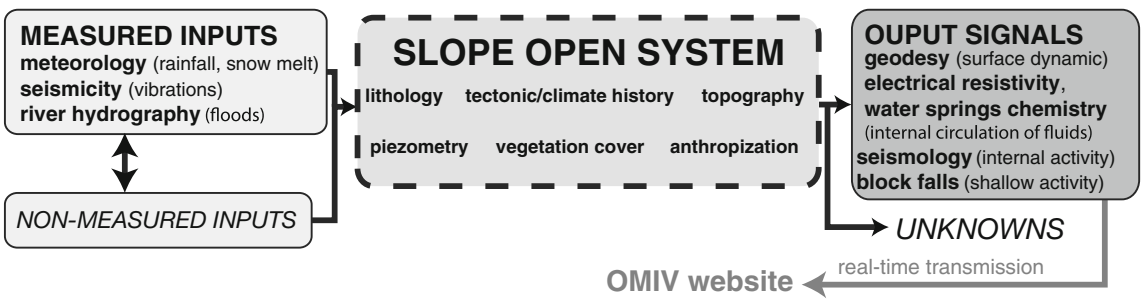

Fig. 4 Conceptual scheme of the different observation components of a slope system

Cartesian coordinates is calculated for each permanent GPS receiver using the SCRS-PPP algorithm. To obtain a centimetric precision with PPP method, some complementary data (IGS products) are introduced in the processing such as precise orbit files (SP3 files), satellite clock bias files (CLK files) and earth rotation parameters files (ERP files). The obtained precise positions are then filtered, smoothed and projected in NTF system. Baselines are also computed between the GPS receivers installed on the landslide (CLP1, CLP2) and the reference receiver (CLAP) installed on stable terrain (Fig. 1) (Malet et al. in review).

These two kinematic references can be used to complete and refine the information given by 68 benchmarks installed from 1982 to 2012 and whose displacement is measured by a permanent total station on the opposite slope (Fig. 2).

Meteorological data

Meteorology, especially rainfall, is the major trigger that mechanically affects shallow geological zones (Caine 1980; Collins and Znidarcic 2004; Guzzetti et al. 2007, 2008; Lebourg et al. 2010; Bernardie et al. 2014; Segoni et al. 2014). Water infiltration in the ground has a strong effect on dilatation of the subsurface material and can reach deeper through fractures. Hence, the meteorological input must be taken into account as a major triggering factor.

Meteorological contributions are the main external input monitored at the study site. Although the presence of snow melt water can only be estimated, quantifying the amount of rainwater available for infiltration is made possible thanks to rain gauge.

Daily rainfall is recorded at the Saint-Etienne-de-Tinée station by Météo-France and is available from 1967. Additionally, three more stations measuring weather conditions at La Clapière have been installed by OMIV in 2011 (Fig. 1). External temperature, rain amounts and intensity, atmospheric pressure, air humidity and wind (average velocity, velocity peak and direction) have been measured at CLAP since 2011 and at CLP2 and CLP3 since 2012.

All the data are sampled every 30 min and transmitted daily via the wireless access point, processed by the Géoazur Laboratory in Nice, and put online (http://omiv.unice.fr/). In this way, we are able to follow in near real time the evolution of weather conditions at three different points in the La Clapière area.

Seismological endogenous events

Although La Clapière DSL does not generate surface flows, it shows a surface activity that can be recorded thanks to a seismological device. To understand the micro-seismic activity related to landslide processes, we deployed a permanent seismological antenna. This device is recording continuously shaking events at the CLP2 (principal lobe) station since 2010. This device consists in six vertical velocity sensors surrounding a three-component Agecodagis NeoMax 4.5 Hz velocimeter. The vertical velocimeters are placed at 50 m from the central three-component velocimeter. All the sensors are buried at 1-m depth and connected to an Agecodagis Kephren receiver. A pseudo-automatic programme has been developed by ISTerre Laboratory of Grenoble in order to detect, locate and classify the events recorded by the station. This classifies discriminate events from their signal characteristics (frequency content, apparent velocity and differentiation of *P* and *S* waves) (Helmstetter and Garambois 2010; Tonnellier et al. 2013). Events are classified in catalogues of events as rockfalls, quakes, earthquakes (including regional and distant) or "not identified" events, that we chose to eliminate from our study.

The local endogenous events (i.e. identified rockfalls and internal quakes located within the landslide area) give us information about the landslide's vibrating state and the surface activity at a given time. These events can be directly related to the rainfall activity, as well as the internal activity of the landslide itself (Helmstetter and Garambois 2010; Tonnellier et al. 2013).

Electrical resistivity measurements

ERT is normally used to image the internal structure of shallow earth. More specifically, it can provide 2D or 3D images of the distribution of electrical resistivity contrasts of the ground. These contrasts are mainly due to differences in lithology and/or to changes in water content but can also be influenced by the ground surface temperature or the infiltrated water chemistry.

ERT has been used for several years by many authors for landslide investigation (Lebourg et al. 1999, 2005; Hack 2000; Jongmans and Garambois 2007; Perrone et al. 2014). This imaging technique can also be applied on hard rock material (Meric et al. 2005; Jomard et al. 2010; Le Roux et al. 2011; Zerathe and Lebourg 2012) as well as on soft rock formations (Samouëlian et al. 2005; Jongmans et al. 2009; Lebourg et al. 2010; Grandjean et al. 2011; Chrétien et al. 2013; Bièvre et al. 2015; Gance et al. 2015). For each study case, the aim is to characterize the water content (degree of saturation of the material) within the investigated landslide body, which is a key factor in understanding the evolution of a landslide. Nevertheless, the limitation of this method is still a lack of quantitative information regarding the amount of water content.

Since November 2012, a permanent electrical line is measuring the electrical resistivity on the slope of La Clapière at the CLP3 station (Fig. 1). Forty-eight electrodes are placed orthogonally to the slope (NW–SE) with a 5-m interval between each electrode. A dipole-dipole array is acquired daily using the IRIS Instruments SYSCAL Pro Switch, providing a 2D cross-section profile of the ground.

This device allows us to reach a depth of investigation of approximately 55 m. Thus, as the temperature effects affect the shallow layers, the daily measurement of resistivity contrasts can be considered as the output signal of water content variation at a certain point (here, at the foot of the slope). Furthermore, the dipole-dipole array allows us to highlight vertical structures in the 2D pseudo-section (Loke 1996–2004; Hack 2000; Dahlin and Zhou 2004). This device is useful for recognizing faults and fractures inside the landslide and the variation of water output signal by means of time lapse.

The Res2Dinv algorithm (Loke and Barker 1996), based on an iterative smoothness-constrained least-squared method, was used for the inversion process of the resistivity data to provide qualitative information on the resistivity contrasts. We then chose to use the apparent measured resistivity data for further analysis to avoid the errors in the iteration process. The idea is to highlight resistivity variations accordingly to the only parameter that can change daily. In this way, we led an analysis by means of clusters of the measured apparent resistivity data after a filtration process.

In a dipole-dipole configuration of 48 electrodes, a large number of resistivity datum points (more than 800 after filtering) with 2D coordinates (x,z) is provided. A filtering phase is necessary

before the treatment of resistivity data. This procedure is shown in Fig. 5.

Results of the annual multi-parameter analysis

The interfering influences (e.g. meteorology, seismicity) on the studied system modify its balance and produce important dynamic changes. Water infiltration is the predominant factor of influence in the case of La Clapière DSL, inducing modification of hydraulic properties and mechanical deformation.

In this study, we observe different signals obtained from the permanent real-time monitoring (Fig. 6). These signals are evidence of specific responses and provide different levels of information on the landslide dynamics, its capacity to respond to a pluviometric event or other.

Geodetic data

Displacements have been observed on the landslide since 1982 (Fig. 2). Figure 7 presents more than 11 years of survey data from 2003 to 2015 thanks to the two GPS installed within the moving mass. From the beginning of the monitoring, CLP2 has moved more than 10 m, whereas CLP1 is now almost 23 m from its original location.

The curves show different behaviours. First, if we focus on the general kinematics, we can observe that the distances between CLAP and CLP1 and between CLAP and CLP2 are in a permanent dynamic evolution. Moreover, the distance between the moving stations and the stable station is decreasing, meaning that the displacement occurs towards CLAP. Eventually, we find a mean displacement over the 2003–2015 period of approximately 2.4 mm day^{-1} for CLP2 and 5.4 mm day^{-1} for CLP1, i.e. a

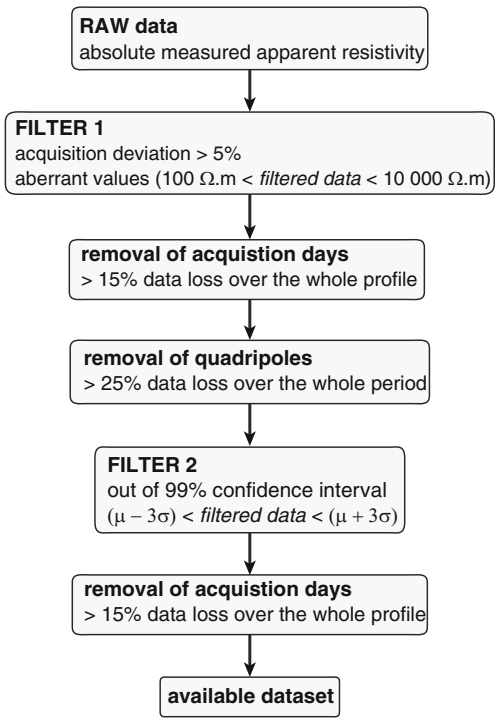

Fig. 5 Diagram of the filtration procedure. The acquisition deviation (quality factor) accounts for the repeatability of these measurements (data quality is improved by stacking at least five measurements for each quadripole

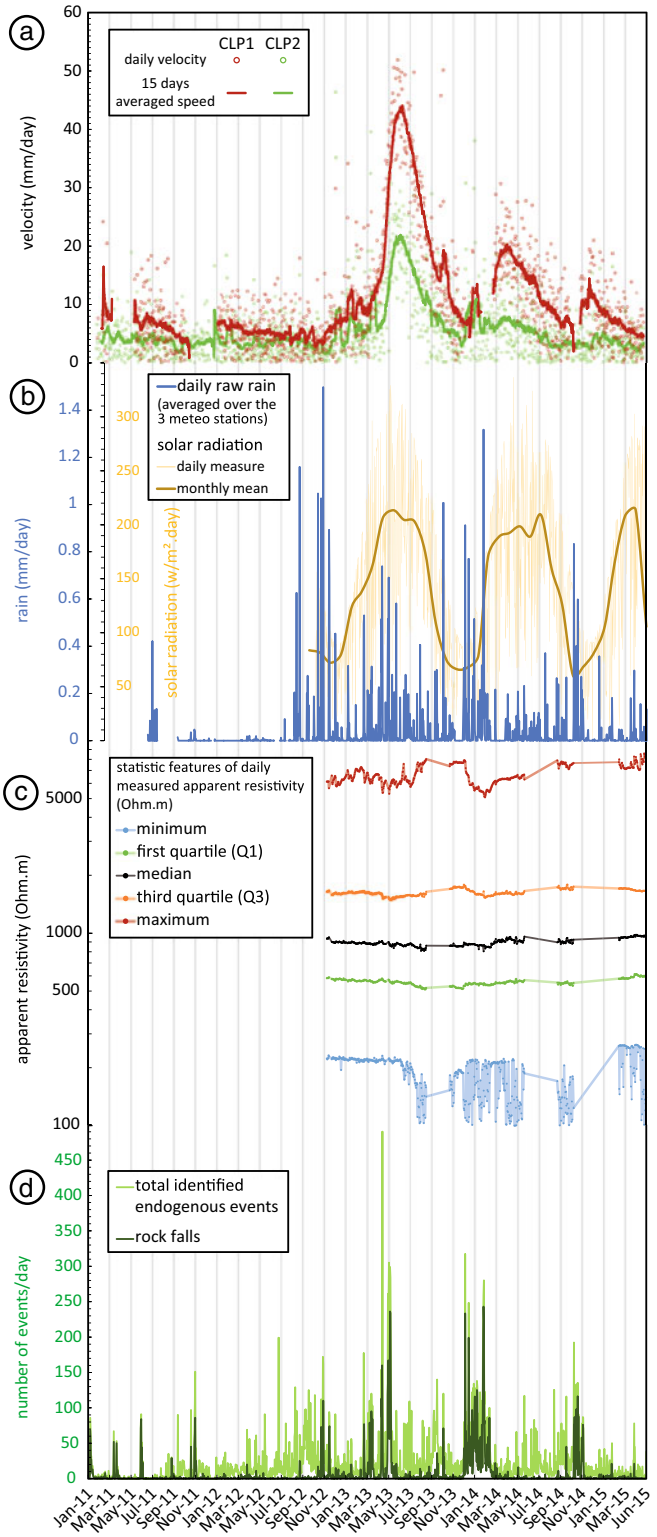

Fig. 6 Multi-parameter observations measured at La Clapière from January 2011 to June 2015. **a** Evolution of the surface velocity of the two moving GPS stations installed at La Clapière. **b** Meteorological features. **c** Evolution of the statistic features of the daily apparent resistivity measured thanks to the ERT profile at CLP3 station. **d** Local endogenous events recorded at La Clapière

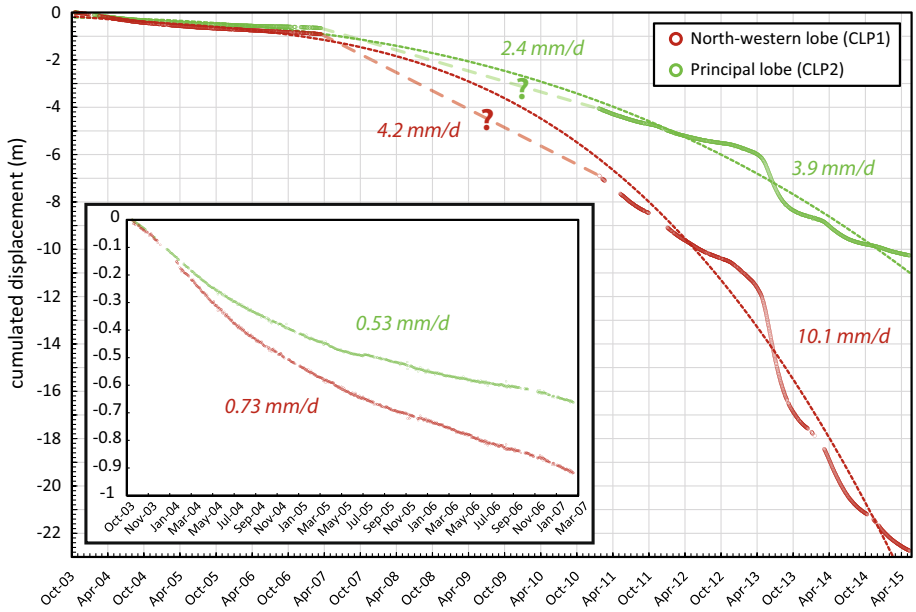

Fig. 7 Evolution of the baselines of the two moving GPS stations installed at La Clapière. Evolution of the distance between CLAP and CLP1 stations (*red dots*). Evolution of the distance between CLAP and CLP2 (*green dots*). The *thick dashed lines* are an estimation of the movement, corresponding to a data gap. The average velocities are also indicated for the different curve portions (2003 to 2007, 2007 to 2011 and 2011 to 2015)

magnitude of 1 to 2 m year^{-1} for the average displacement of this rock slide. The movement occurs towards south-west direction, i.e. perpendicularly to the Tinée River (Fig. 8). According to El Bedoui et al. (2009), the actual mean velocity makes the La Clapière DSL an active to very active landslide.

Second, in addition to the general movement, we observe periods of change in the displacement rates. The curves show a typical "S-shaped" fit, where the distance is decreasing over a relatively short period (Fig. 7). These changes, called "regime" changes, correspond to acceleration phases of the landslide. For example, for the period from May 2013 to August 2013, the displacement of the mobile stations increased significantly: The general velocity of the CLP1 station changed from 5.8 mm day^{-1} to approximately 37.6 mm day^{-1} (i.e. a 6.5-fold increase) and from 5.6 to 18.5 mm day^{-1} for CLP2 (i.e. a 3.3-fold increase) (Figs. 6 and 7). We can note here that the displacement recorded after this regime change has a greater velocity than before it.

In summary, we have two observation levels: (i) "permanent movement" (general displacement) and (ii) "transitory movement" (dynamic changes). Thereafter, in the following sections, we aim at observe and characterize these dynamic changes. More than 2 years of accurate monitoring (November 2012 to December 2014) including dynamic changings mentioned above are presented in order to describe the behaviour of this major landslide.

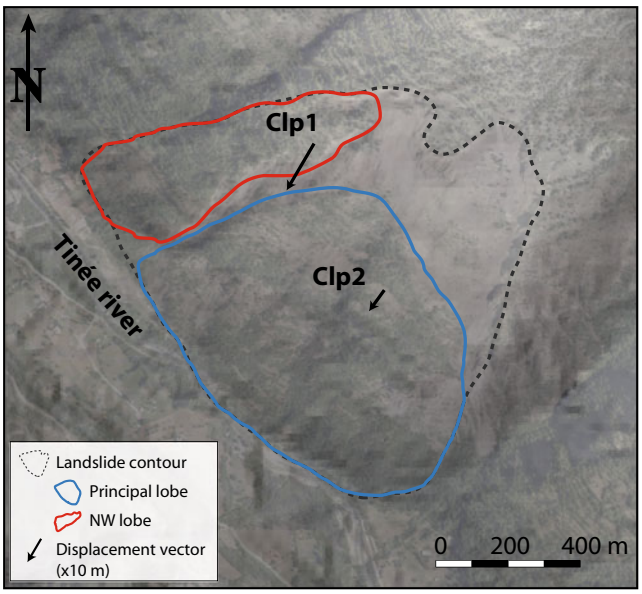

Fig. 8 Displacement of the two GPS stations installed on La Clapière rockslide from 2011 to 2015. The size of the displacement vectors (*black arrows*) has been exaggerated by a factor 10

Relation of rainfall amounts to seismologic endogenous events

Caine (1980) was the first to define global threshold for rainfall triggering shallow landslides and debris flows, using intensity of a rainfall event as a function of its duration associated to the occurrence of landslides. All events occurred above the threshold I_r (in mm h^{-1}) defined by $I_r = 14.82D^{-0.39}$, where D is the event duration, in hours. La Clapière slope is not affected by surface flows but by a movement of the whole mass. Moreover, all the rainfall events recorded in the area are located under Caine's intensity-duration (ID) threshold in such a diagram, where each rainfall event is considered finished as soon as there is a gap of 24 h without rain (Fig. 9).

Endogenous events recorded by the seismological antenna at the CLP2 location inform us about the instantaneous slope activity. To highlight the link between meteorological input and rockfall

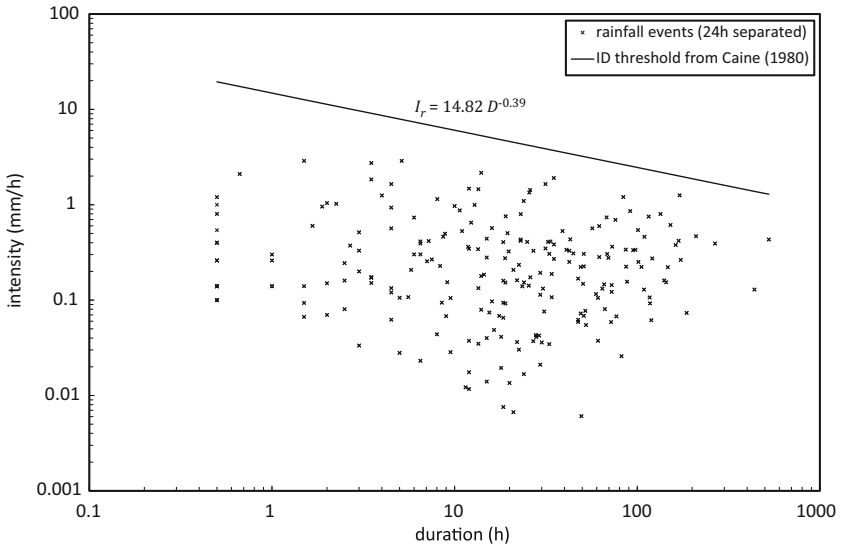

Fig. 9 Features of rainfall events recorded at La Clapière. Caine's ID threshold (1980) is indicated as a *black line*

activity, we use the cumulative rainfall index P_c at time t_i defined by Helmstetter and Garambois (2010):

$$P_c(t_i) = \sum_{j=0:} P(t_j) \exp\left(-\frac{t_i - t_j}{t_c}\right) \quad (1)$$

where the sum of the previous rainfall decreases exponentially with time. This model takes into account the amount of water available for infiltration, decreasing with time due to drainage. We tested different characteristic times ($t_c = 0.25$, 0.5 and 1). The results are similar and show a good fit of precipitation calculated thanks to the cumulative rainfall index and the number of rockfall per day from November 2011 to December 2014 (Fig. 10).

Looking at the cumulated number of endogenous events, the link with rainfall regime appears clear (Fig. 11).

When a period of high rain rate is reached, endogenous activity (mainly surface activity such as rockfalls) increases instantaneously. On the other hand, when the rain activity is poor, endogenous activity remains quite stable. Looking at the period from November 2011 to December 2014, we distinguish three periods of intense rain regime over several weeks generating rapid increase of endogenous events. These periods of high atmospheric activity influence the equilibrium state of the La Clapière natural system, producing surface collapses mostly (rockfalls).

Moreover, the number of daily endogenous seismic events is a good proxy to determine rainfall threshold affecting the state of activity of such a DSL. Indeed, from Fig. 11, we can calculate for each high and low rainfall period an average value linking the intensity of the rain to the number of endogenous events that occurred consecutively from each of these periods (Fig. 12). This figure strongly suggests the existence, in the case of La Clapière, of a rainfall threshold of 3.51 mm day^{-1} from which the number of seismic endogenous events is multiplied at least twice or more.

Link between electrical resistivity and meteorological stress

The area is subject to major rainfall during the year, with the seasonal variability of a temperate zone; there are periods of several days of continuous rain during spring and isolated peaks of high rainfall (up to 4 mm in 30 min) during the summer period. This is a typical Mediterranean mountainous climate, with large variations in rainfall intensity. During the period from the 1 of January 2013 to the 1 of January 2014, a total rainfall amount of 841 mm was recorded at CLAP, 909 mm at CLP2 and 877 mm at CLP3, being a rain amount of 875.8 mm for the year 2013, Saint-Etienne-de-Tinée having an average amount of rain of 949 mm year^{-1} (Météo-France; OMIV).

Considering these various rainfall amounts, we want to observe how the fluids interact with the ground and how they can affect the acceleration of the movement. Because of the continuous motion of the slope, the landslide is not equipped with boreholes, making the installation of piezometers impossible. As a result, we need to observe the circulation of the water inside the moving body using electrical resistivity tomography.

The permanent electrical line installed at the foot of the landslide allows a daily acquisition and makes possible the observation of the evolution of resistivity contrasts in time as a time series of 2D apparent resistivity profiles over a 1-year period. We have noted that the median value of resistivity of the whole data set of a daily profile can provide information about the general resistivity response of the landslide's foot and shows two kinds of interesting variations in time (Figs. 6 and 13).

We observe different variability for the daily apparent resistivity median values, corresponding to two observation scales.

- First, a short period of variability is noted with synchronous steep decreases induced by high rainfall peaks. This is interpreted by a rapid water infiltration affecting the ground resistivity. The main issues here are (1) the amplitude and time

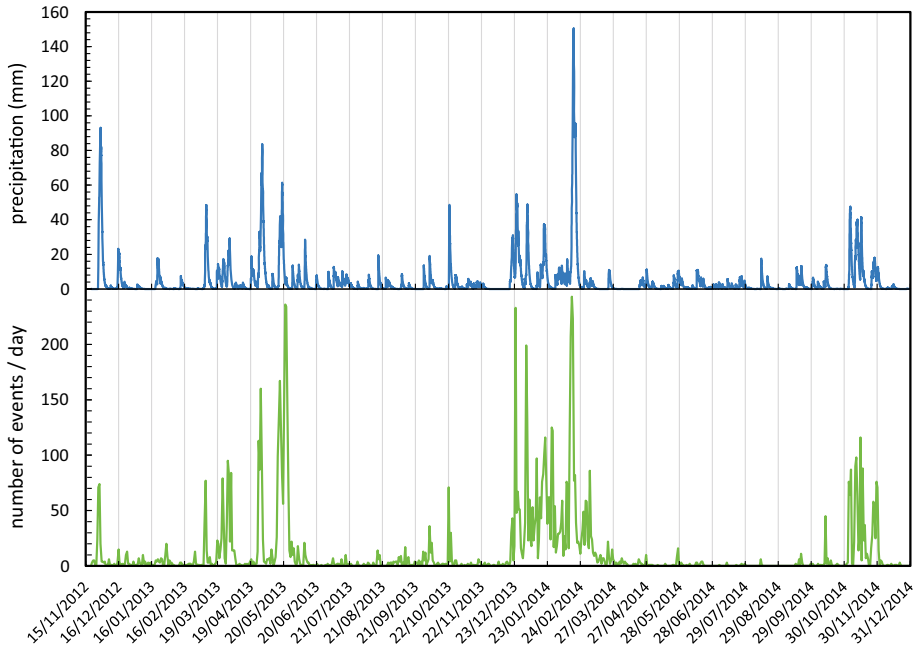

Fig. 10 Precipitation calculated with the cumulative rainfall index of Helmstetter and Garambois (2010) (*top*; *red line*) with $t_c = 1$ day and the number of daily rockfall events (*bottom*; *green line*) recorded at CLP2 seismological station (Fig. 1)

reaction of the measured resistivity on rainfall peaks and (2) the internal areas affected by resistivity contrast decreases induced by water infiltration at a certain moment.

– Secondly, we observe a longer, yearly, period of variation. We have noticed that this frequency seems to be negatively correlated with the variation of the solar radiation recorded at CLP2. Indeed, in addition to the day/night variability, this meteorological parameter shows a clear seasonal variation in the monthly median values (Fig. 6). During wintertime, when average solar radiation is low, the median value of resistivity is high, and the opposite is observed during summertime. These variations of solar radiation at this location allow the seasonal snow cycle of precipitation/melt to operate. The measured apparent resistivity thus seems to illustrate this seasonal variability at this site. Moreover, we may be able to explain the decrease in resistivity around March–April 2013 by the fact that

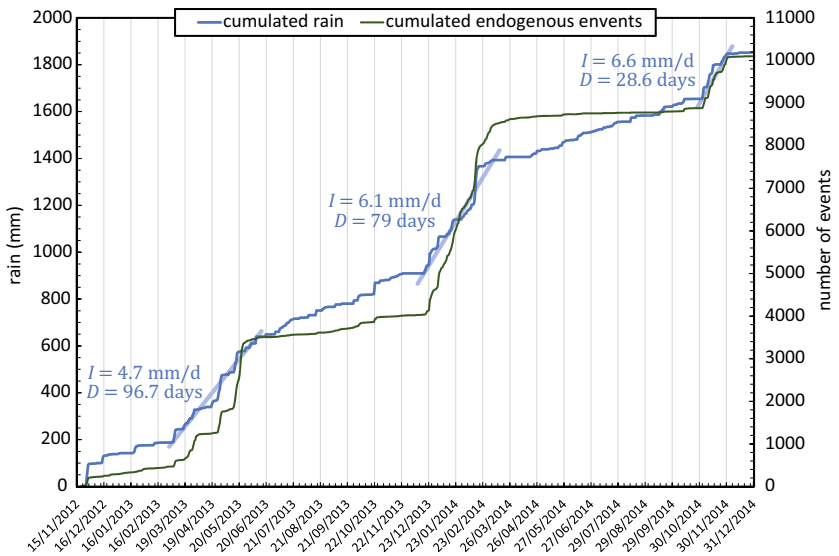

Fig. 11 Curve of cumulated number of daily endogenous events (internal quakes and rockfalls) recorded at CLP2 (*green line*) and cumulated daily rainfall averaged over the three meteorological stations (Fig. 1) (*blue line*). Linear interpolations of high rate of rainfall activity are also indicated, and intensity (I) and duration (D) of these events have been calculated

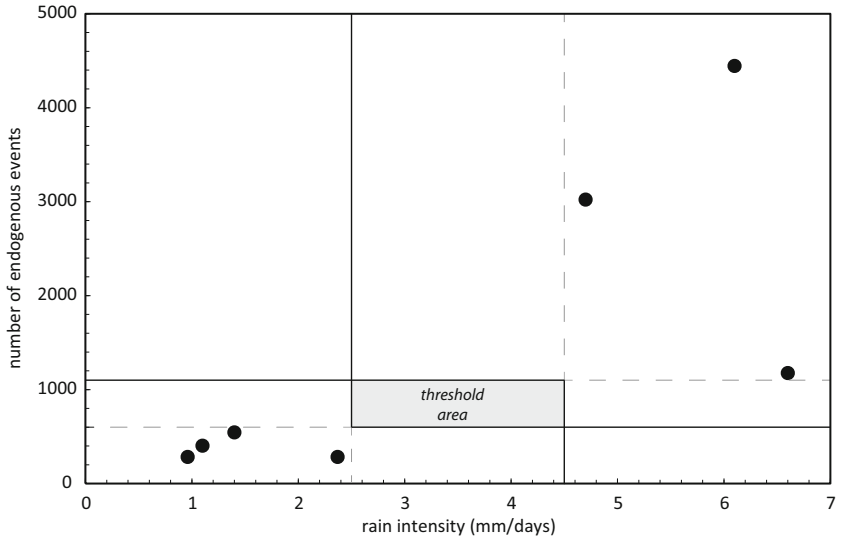

Fig. 12 Diagram of the number of seismic endogenous events as a function of rain intensity for the high and low rainfall periods deduced from Fig. 11

the snow cover accumulated over the La Clapière slope during winter melts at this time of year, when the solar radiation begins to increase significantly. Then, the increase in apparent resistivity values at the end of summertime might be explained by the dryness of the bulk ground, which reduces the conductivity of the buried material.

Discussion

Control of the resistivity signal

The values of resistivity along an electric line for a 1-year period can be very different in space and in time. In fact, we observe different areas within the electrical resistivity section. The different geological compartments of the investigated slope induce a spatial variability, and temporal variations are due to the interaction of the inputs (mainly meteoric water supplies) with these ground compartments.

As data acquisition occurs daily, analysing the correlation coefficient between the point clouds of two consecutive days can yield information about the piezometry level inside the slope (Lebourg et al. 2010).

Evolution of calculated resistivity: pseudo-3D

Another way to visualize the evolution of resistivity in time is through the elaboration of a temporal pseudo-3D visualization.

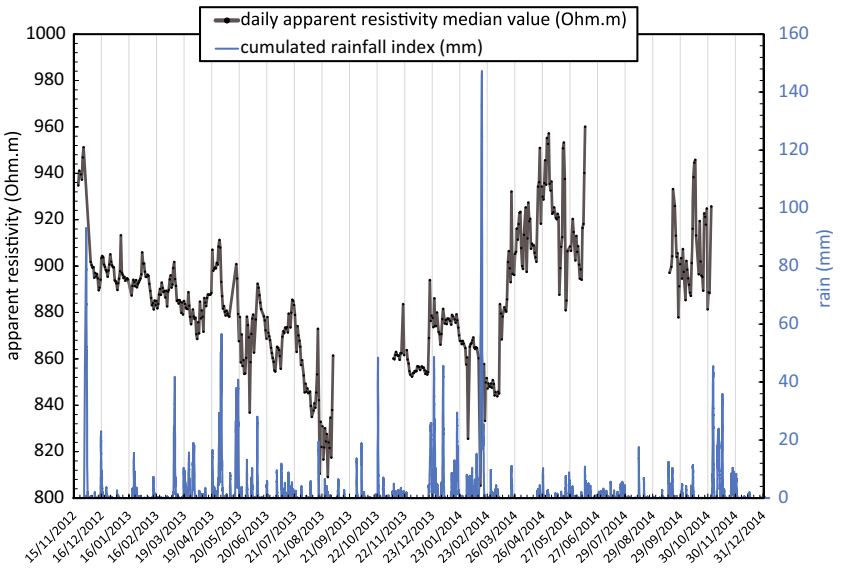

Fig. 13 Time series of precipitations calculated with the cumulative rainfall index of Helmstetter and Garambois (2010) and the daily median value of apparent resistivity profile measured thanks to the ERT profile at CLP3 station

The aim of such an approach is to see how the values of resistivity within the overall 2D sections (x,z) evolve along a time axis (y). This visualization is obtained from the inverted resistivity sections, which inquire into the internal geometry of the slope. The inversions have been done using Res3Dinv (5 % RMS error), where a daily profile corresponds to a unit along the y-axis. Special care has to be taken because this method provides qualitative information and only helps with visualization of the evolution of the resistivity over time.

We can then place the profiles along a virtual temporal axis where unity represents a day. Using 3D software, we can represent an extrapolation of the 1000 Ω m iso-value, which illustrates the evolution in time of the limit of the saturated material for the given period. Figure 14 is an example of 405 days of ERT acquisition in a temporal pseudo-3D representation.

We can first observe that the iso-values at the 25-m depth show a fluctuation of approximately 5 m or more, meaning that the water level in the ground increases and decreases during the year. Second, a small near-surface horizontal zone can be observed between 80 and 140 m along the x-axis. This conductive layer varies laterally, following the level of the bottom conductive layer. Third, a vertical structure (known fault) is clearly visible 90 m from the beginning of the electric line, making a link between the interpreted perched water table and the deep aquifer.

Ranges of apparent resistivity: clusters

The changes between the 2D sections from 1 day to another over several years of monitoring can affect the entire section or be more localized. We then recognize some areas within the ERT section where the values of resistivity vary more or less during the studied period. To study this variability, we chose to group the resistivity data into groups of ranges of electrical resistivity showing the same behaviour. Moreover, clustering these data will help us to understand the responses of these landslide structural elements to external forcing.

In our case, a separation is made between the values above and below 1000 Ω m, a limit corresponding to the base of the landslide. Values lower than 1000 Ω m are mainly located in the lower part of the ERT profile, while those higher than 1000 Ω m are located in the upper part (Table 1, Fig. 15a). We can then assume that the lower part of the profile, which corresponds to the stable bedrock, has a conductive behaviour, an assumption that is in agreement with previous studies (Jomard et al. 2007, 2010).

Thus, we have different areas of different variability with wide ranges of resistivity. This means that the resistivity responds to external forcing and we can directly appreciate its effect within the ground. Moreover, we can distinguish different behaviours corresponding to different geological compartments of the ground.

To enhance the localized variability of resistivity, we use the response of the two main clusters A and B to the rain for this 1-year period (Fig. 15b).

Clusters show different information:

- Cluster B (average resistivity higher than 1000 Ω m, shallow zone of the section) exhibits a very similar variation to the average daily resistivity, indicating that this cluster participates more in the variability of the whole resistivity than cluster A. As expected, cluster B reacts to the rainfall peaks by decreasing very quickly.
- The response to external forcing (rainfall in this case) is clearly not the same for cluster A (average resistivity lower than 1000 Ω m, deep zone of the section). Whereas this cluster exhibits short-term variability, which is seemingly linked to the rainfall peaks (similar to cluster B), the response is less instantaneous. Indeed, the decrease in resistivity after a period of high rainfall is not as steep as for cluster B and seems to be shifted by several days. In this case, the infiltration time can explain this difference in response.

If we look at a longer period, both clusters vary at a seasonal scale. From November to March, cluster A decreases slightly while cluster B increases; then, during the spring (from March to May), cluster B exhibits a widespread decrease while cluster A seems to stay quite stable, with small variations. It is during this period of the year that the most continuous rainfall is recorded, with major

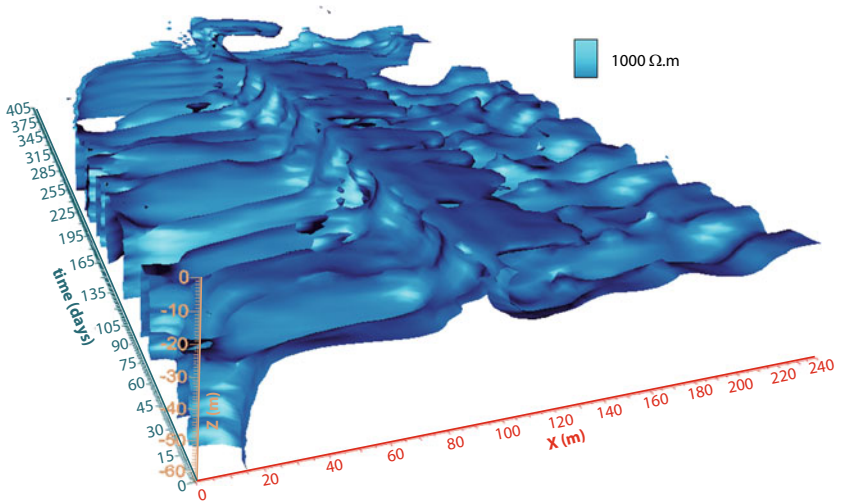

Fig. 14 View of the shape of the 1000 Ω m iso-value in temporal pseudo-3D of the inverted ERT data. This images show the evolution in time of the depth of the upper limit of the saturated zone

Table 1 Statistical features of the two clusters of apparent resistivity in the 1-year average profile, corresponding to two identified areas in the pseudo-section

1-year averaged profile	Cluster A	Cluster B
Average (Ω m)	(<1000 Ω m)	(>1000 Ω m)
	579.4	1894.8
Number of points	477	401

peaks of rain. Finally, from May to December, cluster B increases strongly, unlike cluster A which decreases. The data gap from September to November may, however, distort these observations.

Determination of reactional delay of the slope

We have seen that external factors, especially meteorological factors, influence the destabilization of a weathered slope. We have also assumed that the signals measured by the devices (GPS, ERT, endogenous events) correspond to dynamic features of the slope. One challenge in studying slope movement is to understand how the slope responds to such forcing.

Figure 16 shows the curves of different parameters measured on La Clapière slope along the same temporal axis from November 2012 to December 2014. This allows us to appreciate the joint evolution of raw rainfall and the absolute displacement of the GPS at CLP1 and CLP2.

The S-shaped behaviour of the GPS curves is observed for the cumulated rain curve, but the raw precipitation regime changes, identified thanks to the correlation with the variation of local endogenous events (Figs. 10 and 11), appear several days before the changes are observed in the GPS curves. Moreover, the changes in the GPS kinematics seem to be gentler than the changes of precipitation regime (Fig. 16). Thus, we are able to estimate the general velocities of the GPS movements (Table 2) as well as the rainfall rates of the near-constant rain regimes (Table 3).

We then distinguish two GPS signals (slow and fast) and two rainfall regimes (low and high). Considering the offsets between these curves, we are able to estimate the response times of the GPS movement to the rain stress, as well as the duration of the transition between two speed regimes (Table 4). We interpret that the response time of the slope movement can be calculated as the time between the beginning of a new rainfall regime (high/low) and the subsequent GPS dynamic change (slow/fast). The duration of a regime change is the number of days between two consecutive linear portions of the GPS curves. We can also note that high rainfall regimes are preceded by several days (2 to 3 weeks) without rainfall, making the conditions of saturation very low.

We can confirm here that a period of intense rainfall induces an increase of the displacement rates. However, this dynamic change is not instantaneous but is delayed with respect to the beginning of the rainy period. Moreover, we can note different features of timing in these dynamic changes: (i) Accelerations seem to last for a shorter time than decelerations: In average, a deceleration lasts more than three times an acceleration (accelerations last 3 weeks for the central lobe and up to 7 weeks for the north-western lobe, against more than 3 months for the decelerations, in average), and (ii) the response times are in the range of several weeks (3 weeks for acceleration at the north-western lobe to almost 2 months for deceleration at the central lobe). As a consequence, we can say that the slope seems to respond faster to intense rainfall than to a gentle regime of precipitation: Taking into account the rain regime, an acceleration will appear, in average, 1.5 times faster than a deceleration.

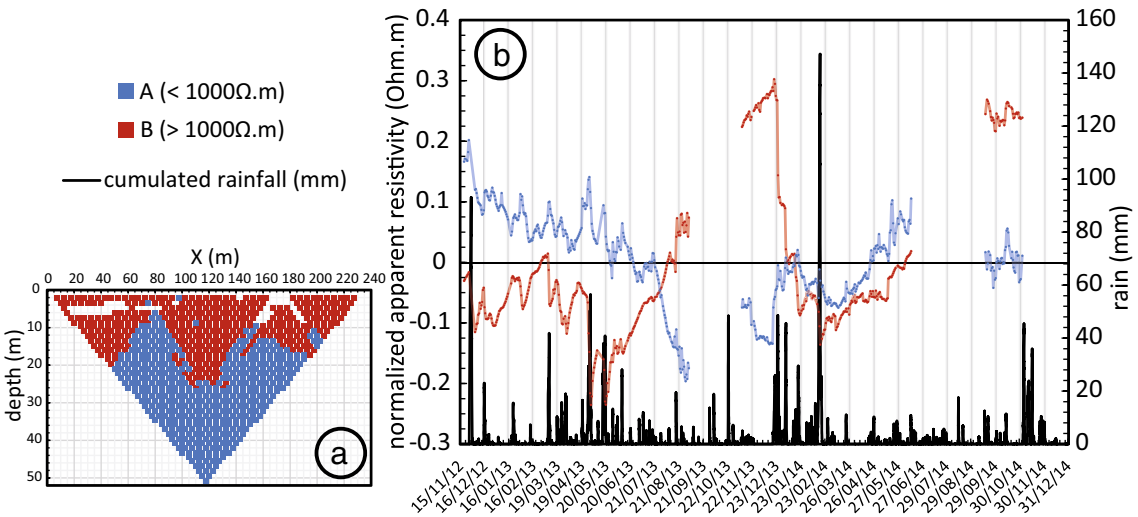

Fig. 15 **a** Localization of the two clusters in the average profile of measured apparent resistivity. *Blue*: cluster A. *Red*: cluster B. **b** Variation of normalized daily average resistivity values of the two clusters (*blue*: A; *red*: B) and the calculated cumulative precipitation from Helmstetter and Garambois (2010) at La Clapière (black) from November 2012 to December 2014

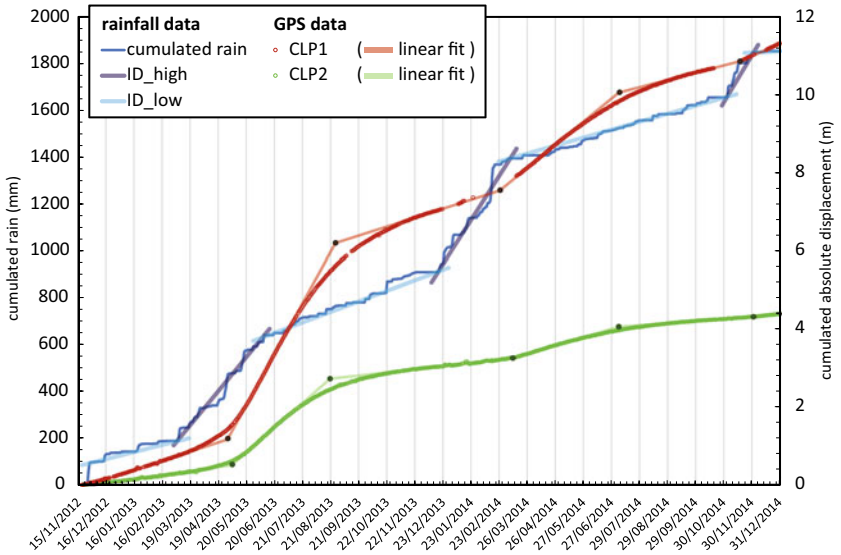

Fig. 16 Evolution of different parameters measured at La Clapière from November 2012 to December 2014

We also note a remarkable difference between the two monitored parts of the landslide. The CLP1 GPS, situated in the north-western part, shows signs of more active displacement than CLP2: For the acceleration and deceleration phases, the north-west lobe reacts 1 to 3 weeks before the principal lobe (Table 4). Additionally, the transition between the two stable dynamic regimes lasts more than 2 weeks longer at CLP1 than CLP2. Finally, we can say that the north-west lobe of La Clapière is more subject to destabilization than the principal lobe. This observation is a new feature of La Clapière DSL regarding the historical velocity trends (Fig. 2). Indeed, the north-west lobe has become more active than the principal lobe since early 2010s. We interpret this new feature as an active lateral extension of the DSL.

Conclusion

A multi-parametric analysis is now essential and should permit us to distinguish the main parameters involved in the destabilization to better characterize the "life" of a landslide and if possible prevent breaks in the dynamics of the process. In our study, we have demonstrated that the use of various tools allows us to observe the behavioural parameters of the La Clapière landslide. For the first time for such a rock slide, over 2 years' accurate data and over 33 years of partial data have been collected and analysed.

First of all, the recording of seismic endogenous events has allowed us to recognized specific features of the rainfall regimes affecting the slope. In this way, periods were identified of several weeks of high rainfall activity producing a significant increase of rockfalls, inducing the establishment of a threshold approximation around 3.5 ± 1 mm day^{-1} of rain activity during several weeks.

Then, the GPS stations installed within the moving mass permitted us to appreciate the way the geological object is moving as a whole. This is a useful tool to see the "general" movement of a landslide. When analysing in detail the La Clapière dynamic evolution, typical changes were observed in the velocity that we called "dynamic regime changes". Thus, we can consider three possible behaviours after a regime change: (i) the system regains its previous velocity; (ii) the velocity of displacement is greater than before, and destabilization takes place or (iii) the velocity of displacement is less than before the change, and the system reaches a level of stabilization. Moreover, accelerations appear to occur within a shorter time period than decelerations. Furthermore, thanks to two GPS bases on two distinct parts of

Table 2 Features of the linear portions of the GPS curves

Moving regime	Period (±2 days)		Velocity (mm day^{-1})	
	CLP1	CLP2	CLP1	CLP2
Slow	20 Nov. 2012–17 Mar. 2013	20 Nov. 2012–10 Apr. 2013	7.1	3.0
Fast	20 May 2013–06 Jul. 2013	18 May 2013–13 Jul. 2013	41.8	20.3
Slow	05 Nov. 2013–26 Jan. 2014	22 Oct. 2013–04 Mar. 2014	8.3	2.9
Fast	19 Mar. 2014–20 May 2014	16 Mar. 2014–01 Jun. 2014	18.4	6.7
Slow	29 Aug. 2014–19 Oct. 2014	20 Aug. 2014–23 Nov. 2014	6.2	1.8
Fast	20 Nov. 2014–31 Dec. 2014	11 Dec. 2014–31 Dec. 2014	10.4	2.5

Table 3 Features of rainfall curves

Rainfall regime	Period	Rain intensity (mm day^{-1})	Period duration (days)
Low	29 Nov. 2012–05 Mar. 2013	0.96	95.7
High	05 Mar. 2013–10 Jun. 2013	4.7	96.7
Low	10 Jun. 2013–19 Dec. 2013	1.4	270.6
High	19 Dec. 2013–08 Mar. 2014	6.1	79
Low	08 Mar. 2014–03 Nov. 2014	1.1	240
High	03 Nov. 2014–02 Dec. 2014	6.6	28.6
Low	From 02 Dec. 2014	0.037	>29

the landslide (north-western and principal lobes, Figs. 1 and 8), the differences in displacement between these two landslide compartments have been measured.

To understand the origins of these changes, we observed how the external forcing and internal features were related. We have thus seen that the main forcing is the atmospheric events. In addition, these external inputs affect the whole landslide. The main result of this study shows that the regime changes will then appear at the same time, but temporal offsets are detected in the duration and timing of the mentioned events. Thus, a dynamic change at CLP1 lasts 2.5 ± 0.6 months on average compared with 1.9 ± 0.4 months on average at CLP2.

At the scale of the slope, movement's response times to rainfall stress have been determined. Indeed, dynamic regime changes always appear after a period of a particular rainfall pattern: acceleration after high rainfall and deceleration after low intensity rainfall period. This delay is on the order of a week or more in magnitude and is smaller at CLP1 (5.1 ± 2.6 weeks) than at CLP2 (7.4 ± 3.5 weeks).

The measured resistivity of the ground responds much more rapidly to meteorological forcing. The installation of a permanent ERT line allowed us to obtain a scalable pseudo-section in time. Thus, it is possible to highlight different behavioural trends within the pseudo-section. The established clusters can be differentiated into two main groups: (i) from 0 to 20 m depth, high resistivities (cluster B) are highly negatively correlated with rainfall peaks; (ii) from 20 to 50 m depth, low resistivities (cluster A), which correspond to the deep saturated zone, respond more slowly to rain stress and must be drained and fed by the fault located at the left part of the line. In addition, looking at the evolution of the median values of apparent resistivity of each daily measured profile, a larger period of variability can be seen, which may be seasonal and interpreted as the effect of snow melting during spring time, an important phenomenon regarding the geographical situation of the La Clapière slope (mountainous domain).

Finally, the GPS movements measured within the slope have shown that the velocity before and after an acceleration phase is not the same, meaning that the La Clapière DSL is a complex dynamic geological system where many factors influence its evolution and thus presents different equilibrium states in time. Indeed, understanding its behaviour over time remains an important challenge regarding the risk for the nearby Saint-Etienne-de-Tinée village. The permanent stations installed within the slope will allow us to study the evolution of the parameters of influence over an even larger period.

Table 4 Features of the regime changes calculated from Fig. 16

Period	Type of regime change	Duration (±2 days)		Response time to the rain (±2 days)	
		CLP1	CLP2	CLP1	CLP2
March to May 2013	Acceleration	64	38	12	36
July to Nov. 2013	Deceleration	122	101	26	33
Feb. to March 2014	Acceleration	$48 < t < 52$	12	$38 < t < 44$	75
May to Aug. 20144	Deceleration	101	80	73	85
Nov. 2014	Acceleration	$6 < t < 32$	18	<11	20
Average (±4 days)	Acceleration	$39 < t < 49$	23	<22	44
	Deceleration	112	91	50	59
Standard deviation (±4 days)	Acceleration	$13 < t < 24$	11	>12	23
	Deceleration	11	11	24	26

These could then be integrated into new models of prediction and more effective alarm systems.

Acknowledgments

This work is supported by PACA Region, OCA Observatory and INSU OMIV project (Landslides French Observatory).

References

Bernardie S, Desramaut N, Malet J-P, Gourlay M, Granjean G (2014) Prediction of changes in landslide rates induced by rainfall. Landslides. doi:10.1007/s10346-014-0495-8

Bièvre G, Jongmans D, Goutaland D, Pathier E, Zumbo V (2015) Geophysical characterization of the lithological control on the kinematic pattern in a large clayey landslide (Avignonet, French Alps). Landslides. doi:10.1007/s10346-015-0579-0

Bigot-Cormier F, Poupeau G, Sosson M (2000) Dénudations différentielles du massif cristallin externe alpin de l'Argentera (Sud-Est de la France) relevées par thermochronologie traces de fission (apatites, zircons). C R Acad Sci Paris Sci de la Terre et des planètes Earth Planet Sci 330:363–370

Bigot-Cormier F, Braucher R, Burlès D, Guglielmi Y, Dubar M, Stéphan J-F (2005) Chronological constraints on processes leading to large active landslides. Earth Planet Sci Lett 235:141–150. doi:10.1016/j.epsl2005.03.012

Bigot-Cormier F, Sosson M, Poupeau G, Stéphan J-F, Labrin E (2006) The denudation history of the Argentera Alpine External Crystalline Massif (Western Alps, France-Italy): an overview from the analysis of fission tracks in apatites and zircons. Geodin Acta 19(6):455–473

Binet S, Jomard H, Lebourg T, Guglielmi Y, Tric E, Bertrand C, Mudry J (2007) Experimental analysis of groundwater and artificial water chemical tracers. Hydrol Process 21:3463–3472. doi:10.1002/hyp.6579

Bogdanoff S (1980) Analyse structurale dans la partie occidentale de l'Arengtera-Mercantour (Alpes Maritimes). Doctoral dissertation, Université Paris Sud-Paris XI

Bogdanoff S, Michard A, Mansour M, Poupeau G (2000) Apatite fission track analysis in the Argentera massif: evidence of contrasting denudation rates in the External Crystalline Massifs of the Western Alps. Terra Nov. 12(3):117–125. doi:10.1046/j.1365-3121.2000.123281.x

Bois T, Bouissou S, Guglielmi Y (2008) Influence of major inherited faults zones on gravitational slope deformation: a two-dimensional physical modelling of the La Clapière area (Southern French Alps). Earth Planet Sci Lett 272:709–719. doi:10.1016/j.epsl.2008.06.006

Bois T, Tric E, Lebourg T (2014) Influence of inherited topography on gravitational slope failure: three-dimensional numerical modelling of the La Clapière slope, Alpes-Maritimes, France. Terra Nov. 26:1–9. doi:10.1111/ter.12105

Booth AM, Lamb MP, Avouac J-P, Delacourt C (2013) Landslide velocity, thickness, and rheology from remote sensing: La Clapière landslide, France. Geophys Res Lett 40:4299–4304. doi:10.1002/grl.50828

Caine N (1980) The rainfall intensity-duration control of shallow landslides and debris flows. Geogr Ann 62A(1–2):23–27

Cappa F, Guglielmi Y, Soukatchoff VM, Mudry J, Bertrand C, Charmoille A (2004) Hydromechanical modeling of a large moving rock slope inferred from slope levelling coupled to spring long-term hydrochemical monitoring: example of the La Clapière landslide (Southern Alps, France). J Hydrol 291:67–90. doi:10.1016/j.jhydrol.2003.12.013

Casson B, Delacourt C, Baratoux D, Allemand P (2003) Seventeen years of the "La Clapière" landslide evolution analysed from ortho-rectified aerial photographs. Eng Geol 68:123–139

Chrétien M, Lataste J-F, Fabre R, Denis A (2013) Electrical resistivity tomography to understand clay behavior during seasonal water content variations. Eng Geol. doi:10.1016/j.enggeo.2013.11.019

Collins BD, Znidarcic D (2004) Stability analyses of rainfall-induced landslides. J Geotech Geoenviron 130(4):362–372. doi:10.1061/(ASCE)1090-0241(2004)130:4(362)

Compagnon F, Guglielmi Y, Mudry J, Follacci J-P, Ivaldi J-P (1997) Approche chimique et isotopique de l'origine des eaux en transit dans un grand mouvement de terrain: exemple du glissement de La Clapière (Alpes-Maritimes, France). Comptes Rendus de l'Acad des Sci Ser IIA Earth Planet Sci 325(8):565–570. doi:10.1016/S1251-8050(97)89456-6

Corsini M, Ruffet G, Caby R (2004) Alpine and late-Hercynian geochronological constraints in the Argentera Massif (Western Alps). Eclogae Geol Helv 97:3–15. doi:10.1007/s00015-004-1107-8

Crosta GB (1998) Regionalization of rainfall thresholds: an aid to landslide hazard evaluation. Environ Geol 35(2–3):131–145. doi:10.1007/s002540050300

Crosta GB, di Prisco C, Frattini P, Frigerio G, Castellanza R, Agliardi F (2014) Chasing a complete understanding of the triggering mechanisms of a large rapidly evolving rockslide. Landslides 11:747–764. doi:10.1007/s10346-013-0433-1

Dahlin T, Zhou B (2004) A numerical comparison of 2D resistivity imaging with 10 electrode arrays. Geophys Prospect 52:379–398

Delacourt C, Allemand P, Berthier E, Raucoules D, Casson B, Grandjean P, Pambrun C, Varel E (2007) Remote-sensing techniques for analysing landslide kinematics: a review. Bull Soc Geol Fr 178(2):89–100. doi:10.2113/gssgfbull.178.2.89

El Bedoui S, Guglielmi Y, Lebourg T, Pérez J-L (2009) Deep-seated failure propagation in a fractured rock slope over 10,000 years: the La Clapière slope, the south-eastern French Alps. Geomorphology 105:232–238. doi:10.1016/j.geomorph.2008.09.025

El Bedoui S, Bois T, Jomard H, Sanchez G, Lebourg T, Tric E, Guglielmi Y, Bouissou S, Chemenda A, Rolland Y, Corsini M, Pérez JL (2011) Paraglacial gravitational deformations in the SW Alps: a review of field investigations, 10Be cosmogenic dating and physical modelling. Geol Soc Lond Spec Publ 351(1):11–25. doi:10.1144/SP351.2

Follacci J-P (1987) Les mouvements du versant de La Clapière à Saint-Etienne-de-Tinée (Alpes-Maritimes). Bull Lab Ponts et Chaussées 220(150–151):107–109

Follacci J-P, Rochet L, Serratrice J-F (1993) Glissement de La Clapière, St. Etienne de Tinée, Synthèse des connaissances et actualisation des risques, rapp. 92/PP/UN/I/DRM/03/AI/01, 76 pp., Cent. Etud. Tech. de l'Equip., Nice, France

Gance J, Sailhac P, Malet J-P (2015) Corrections of surface effect on apparent resistivity measurements. Geophys J Int 200:1118–1135. doi:10.1093/gji/ggu453

Grandjean G, Courry JC, Sanchez O, Bitri A, Garambois S (2011) Structural study of the Ballanz landslide (French Alps) using geophysical imagery. J Appl Geophys 75:537–542. doi:10.1016/j.jappgeo.2011.07.008

Guglielmi Y, Cappa F (2010) Regional-scale relief evolution and large landslides: insights from geomechanical analyses in the Tinée Valley (southern French Alps). Geomorphology 117:121–129. doi:10.1016/j.geomorph.2009.11.016

Guglielmi Y, Vengeon JM, Bertrand C, Mudry J, Follacci JP, Giraud A (2002) Hydrogeochemistry: an investigation tool to evaluate infiltration into large moving rock masses (case study of La Clapière and Séchilienne alpine landslides). Bull Eng Geol Environ 61:311–324. doi:10.1007/s10064-001-0144-z

Gunzburger Y, Laumonier B (2002) Origine tectonique du pli supportant le glissement de terrain de la Clapière (Nord-Ouest du massif de l'Argentera-Mercantour, Alpes du Sud, France) d'après l'analyse de la fracturation. Compt Rendus Geosci 334(6):415–422. doi:10.1016/S1631-0713(02)01761-3

Guzzetti F, Peruccacci S, Rossi M, Stark CP (2007) Rainfall thresholds for the initiation of landslides in central and southern Europe. Meteorog Atmos Phys 98:239–267. doi:10.1007/s00703-007-0262-7

Guzzetti F, Peruccacci S, Rossi M, Stark CP (2008) The rainfall-duration control of shallow landslides and debris flows: an update. Landslides 5(1):3–17. doi:10.1007/s10346-007-0112-1

Hack R (2000) Geophysics for slope stability. Surv Geophys 21:423–448

Helmstetter A, Garambois S (2010) Seismic monitoring of Séchilenne rockslide (French Alps): analysis of seismic signals and their correlation with rainfalls. J Geophys Res 115:F03016. doi:10.1029/2009JF001532

Helmstetter A, Sornette D, Grasso J-R, Andersen JV, Gluzman S, Pisarenko V (2004) Slider block friction model for landslides: application to Vaiont and La Clapière landslides. J Geophys Res 109:B02409. doi:10.1029/2002JB002160

Jaboyedoff M, Oppikofer T, Abellán A, Derron MH, Loye A, Metzger R, Pedrazzini A (2012) Use of LIDAR in landslide investigations: a review. Nat Hazards 61(1):5–28. doi:10.1007/s11069-010-9634-2

Jomard H (2006) Analyse multi-échelles des deformations gravitaires du Massif de l'Argentera Mercantour. Thèse de Doctorat en Sciences de la Terre, Université de Nice Sophia-Antipolis, 217 pp

Jomard H, Lebourg T, Tric E (2007) Identification of the gravitational boundary in weathered gneiss by geophysical survey: La Clapière landslide (France). J Appl Geophys 62:47–57. doi:10.1016/j.jappgeo.2006.07.003

Jomard H, Lebourg T, Guglielmi Y, Tric E (2010) Electrical imaging of sliding geometry and fluids associated with a deep seated landslide (La Clapière, France). Earth Surf Process Landf 35(5):588–599. doi:10.1002/esp.1941

Jomard H, Lebourg T, Guglielmi Y (2013) Morphological analysis of deep-seated gravitational slope deformation (DSGSD) in the western part of the Argentera massif. A morpho-tectonic control? Landslides. doi:10.1007/s10346-013-0434-0

Jongmans D, Garambois S (2007) Geophysical investigation of landslides: a review. Bull Soc Geol Fr 178(2):101–112

Jongmans D, Bièvre G, Renalier F, Schwartz S, Beaurez N, Orengo Y (2009) Geophysical investigation of a large landslide in glaciolacustrine clays in the Trièvres area (French Alps). Eng Geol 109:45–56. doi:10.1016/j.enggeo.2008.10.005

Julian M (1980) Les Alpes Maritimes Franco-Italiennes. Etude géomorphologique. Thèse présentée devant l'Université d'Aix-Marseille II, 26 juin 1976, Volume 2, 836 pp

Julian M, Anthony E (1996) Aspects of landslide activity in the Mercantour Massif and the French Riviera, southeastern France. Geomorphology 15:275–289

Keefer DK (2002) Investigating landslides caused by earthquakes–a historical review. Surv Geophys 23(6):473–510. doi:10.1023/A:1021274710840

Korup O, Clague JJ, Hermanns RL, Hewitt K, Strom AL, Weidinger JT (2007) Giant landslides, topography, and erosion. Earth Planet Sci Lett 261(3):578–589. doi:10.1016/j.epsl.2007.07.025

Korup O, Densmore AL, Schlunegger F (2010) The role of landslides in mountain range evolution. Geomorphology 120(1):77–90. doi:10.1016/j.geomorph.2009.09.017

Le Roux O, Jongmans D, Kasperski J, Schwartz S, Potherat P, Lebrouc V, Lagabrielle R, Meric O (2011) Deep geophysical investigation of the large Séchilienne landslide (Western Alps, France) and calibration with geological data. Eng Geol 120:18–31. doi:10.1016/j.enggeo.2011.03.004

Lebourg T, Frappa M, Sirieix C (1999) Reconnaissance des surfaces de rupture dans les formations superficielles instables par mesures électriques. PANGEA 31:69–72

Lebourg T, Binet S, Tric E, Jomard H, El Bedoui S (2005) Geophysical survey to estimate the 3D slipping surface and the 4D evolution of the water pressure on part of a deep seated landslide. Terra Nov. 17:399–406. doi:10.1111/j.1365-3121.2005.00623.x

Lebourg T, Hernandez M, Zerathe S, El Bedoui S, Jomard H, Fresia B (2010) Landslides triggered factors analysed by time lapse electrical survey and multidimensional statistical approach. Eng Geol 114:238–250. doi:10.1016/j.enggeo.2010.05.001

Lebourg T, Hernandez M, Jomard H, El Bedoui S, Bois T, Zerathe S, Tric E, Vidal M (2011) Temporal evolution of weathered cataclastic material in gravitational faults of the La Clapière deep-seated landslide by mechanical approach. Landslides. doi:10.1007/s10346-010-0244-6

Loke MH (1996–2014) Tutorials: 2-D and 3-D electrical imaging surveys, www.geoelectrical.com, 169 pp

Loke MH, Barker RD (1996) Rapid least-squares inversion of apparent resistivity pseudosections by a quasi-Newton method. Geophys Prospect 44:131–152. doi:10.1111/j.1365-2478.1996.tb00142.x

Macfarlane DF (2009) Observations and predictions of the behaviour of large, slow-moving landslides in schist, Clyde Dam reservoir, New Zealand. Eng Geol 109:5–15. doi:10.1016/j.enggeo.2009.02.005

Mainsant G, Larose E, Brönnimann C, Jongmans D, Michoud C, Jaboyedoff M (2012) Ambient seismic noise monitoring of a clay landslide: Toward failure prediction. J Geophys Res 117:F01030. doi:10.1029/2011JF002159

Malet J-P, Boetzlé P, Ferhat G, Masson F, Ulrich P, (subm) Evaluation of different processing strategies of Continuous GPS (CGPS) observations for long-term landslide monitoring. J Geodesy, 24p. (in review)

Meric O, Garambois S, Jongmans D, Wathelet M, Chatelain JL, Vengeon JM (2005) Application of geophysical methods for the investigation of large gravitational mass movement of Séchilienne, France. Can Geotech J 42:1105–1115. doi:10.1139/T05-034

Musumeci G, Ribolini A, Spagnolo M (2003) The effects of late Alpine tectonics in the morphology of the Argentera Massif (Western Alps, Italy-France). Quat Int 101–102:191–201

Perrone A, Lapenna V, Piscitelli S (2014) Electrical tomography technique for landslide investigations: a review. Earth-Sci Rev. doi:10.1016/j.earscirev.2014.04.002

Prokešová R, Kardoš M, Táborík P, Medved'ová A, Stacke V, Chudý F (2014) Kinematic behaviour of a large earthflow defined by surface displacement monitoring, DEM differencing, and ERT imaging. Geomorphology 224:86–101. doi:10.1016/j.geomorph.2014.06.029

Samouëlian A, Cousin I, Tabbagh A, Bruand A, Richard G (2005) Electrical resistivity survey in soil science. Soil Tillage Res 83:173–193. doi:10.1016/j.still.2004.10.004

Schlögel R, Doubre C, Malet J-P, Masson F (2015a) Landslide deformation monitoring with ALOS/PALSAR imagery: a D-InSAR geomorphological interpretation method. Geomorphology 231:314–330. doi:10.1016/j.geomorph.2014.11.031

Schlögel R, Malet J-P, Doubre C, Lebourg T (2015b) Structural control on the kinematics of the deep-seated La Clapière landslide revealed by L-band InSAR observations. Landlides 1–14. doi:10.1007/s10346-015-0623-0

Segoni S, Lagomarsino D, Fanti R, Moretti S, Casagli N (2014) Integration of rainfall and susceptibility maps in the Emilia Romagna (Italy) regional-scale landslide warning system. Landslides. doi:10.1007/s10346-014-0502-0

Tonnellier A, Helmstetter A, Malet J-P, Schmittbuhl J, Corsini A, Joswig M (2013) Seismic monitoring of soft-rock landslides: the Super-Sauze and Valoria case studies. Geophys J Int. doi:10.1093/gji/ggt039

Tric E, Lebourg T, Jomard H, Le Cossec J (2010) Study of large-scale deformation induced by gravity on the La Clapière landslide (Saint-Etienne de Tinée, France) using numerical and geophysical approaches. J Appl Geophys 70:206–215. doi:10.1016/j.jappgeo.2009.12.008

Varnes DJ (1978) Slope movement types and processes. In: Schutler RL and Krizek RJ (eds) Landslides: analysis and control. TRB Special Report 176, Washington DC, pp 11–33

Zerathe S, Lebourg T (2012) Evolution stages of large deep-seated landslides at the front of a subalpine meridional chain (Maritime-Alps, France). Geomorphology 138:390–403

E. Palis (✉) · T. Lebourg · E. Tric · M. Vidal
Univ. Nice-Sophia Antipolis, CNRS, IRD, Observatoire de la Côte d'Azur, Géoazur UMR 7329,
250 Avenue Albert Einstein, 06560, Valbonne, France
e-mail: palis@geoazur.unice.fr

J. Malet
Institut de Physique du Globe de Strasbourg, CNRS, UMR 7516/EOST, Université de Strasbourg,
5 rue Descartes, 67084, Strasbourg Cedex, France